# Haemodynamic performance of 16-20-mm extracardiac Goretex conduits in adolescent Fontan patients at rest and during simulated exercise

Rijnberg, F.M.; van't Hul, L.C.; Hazekamp, M.G.; Boogaard, P.J. van den; Juffermans, J.F.; Lamb, H.J.; … ; Wentzel, J.J.

**ORIGINAL ARTICLE**

# Haemodynamic performance of 16–20-mm extracardiac Goretex conduits in adolescent Fontan patients at rest and during simulated exercise

Friso M. Rijnberg [a,*], Luca C. van 't Hul[b], Mark G. Hazekamp[a], Pieter J. van den Boogaard[c],

Joe F. Juffermans[c], Hildo J. Lamb[c], Covadonga Terol Espinosa de Los Monteros[d], Lucia J.M. Kroft[c],

Sasa Kenjeres[e], Saskia le Cessie [f], Monique R.M. Jongbloed[g], Jos J.M. Westenberg [c],

Arno A.W. Roest[d,†] and Jolanda J. Wentzel[b,†]

[a] Department of Cardiothoracic Surgery, Leiden University Medical Center, Leiden, Netherlands
[b] Department of Cardiology, Biomechanical Engineering, Erasmus MC, Rotterdam, Netherlands
[c] Department of Radiology, Leiden University Medical Center, Leiden, Netherlands
[d] Department of Pediatric Cardiology, Leiden University Medical Center, Leiden, Netherlands
[e] Department of Chemical Engineering, Faculty of Applied Sciences, Delft University of Technology and J.M. Burgers centrum Research School for Fluid Mechanics, Delft, Netherlands
[f] Department of Clinical Epidemiology, Leiden University Medical Center, Leiden, Netherlands
[g] Department of Cardiology and Anatomy & Embryology, Leiden University Medical Center, Leiden, Netherlands

* Corresponding author. Department of Cardiothoracic surgery, Leiden University Medical Center, Albinusdreef 2, 2333ZA, Leiden, the Netherlands,
  Email: f.m.rijnberg@lumc.nl Telephone number:+31715262348 (F.M. Rijnberg).

**Key question**

What is the hemodynamic performance of the TCPC in older Fontan patients with 16-20mm extracardiac conduits?

**Key finding(s)**

An extracardiac conduit ≤45mm$^2$/L/min is associated with adverse hemodynamics and >125mm$^2$/L/min with favorable hemodynamics. TCPC resistance correlated with peak VO2.

**Take-home message**

16-20mm conduits become relatively undersized in most adolescent Fontan patients leading to suboptimal TCPC hemodynamics, especially during increased flow conditions.

†These authors shared the senior authorship.

## Abstract

**OBJECTIVES:** To date, it is not known if 16–20-mm extracardiac conduits are outgrown during somatic growth from childhood to adolescence. This study aims to determine total cavopulmonary connection (TCPC) haemodynamics in adolescent Fontan patients at rest and during simulated exercise and to assess the relationship between conduit size and haemodynamics.

**METHODS:** Patient-specific, magnetic resonance imaging-based computational fluid dynamic models of the TCPC were performed in 51 extracardiac Fontan patients with 16–20-mm conduits. Power loss, pressure gradient and normalized resistance were quantified in rest and during simulated exercise. The cross-sectional area (CSA) (mean and minimum) of the vessels of the TCPC was determined and normalized for flow rate ($mm^2$/l/min). Peak (predicted) oxygen uptake was assessed.

**RESULTS:** The median age was 16.2 years (Q1–Q3 14.0–18.2). The normalized mean conduit CSA was 35–73% smaller compared to the inferior and superior vena cava, hepatic veins and left/right pulmonary artery (all $P < 0.001$). The median TCPC pressure gradient was 0.7 mmHg (Q1–Q3 0.5–0.8) and 2.0 (Q1–Q3 1.4–2.6) during rest and simulated exercise, respectively. A moderate–strong inverse non-linear relationship was present between normalized mean conduit CSA and TCPC haemodynamics in rest and exercise. TCPC pressure gradients of $\geq 1.0$ at rest and $\geq 3.0$ mmHg during simulated exercise were observed in patients with a conduit CSA $\leq 45$ $mm^2$/l/min and favourable haemodynamics (<1 mmHg during both rest and exercise) in conduits $\geq 125$ $mm^2$/l/min. Normalized TCPC resistance correlated with (predicted) peak oxygen uptake.

**CONCLUSIONS:** Extracardiac conduits of 16–20 mm have become relatively undersized in most adolescent Fontan patients leading to suboptimal haemodynamics.

**Keywords:** Fontan • Total cavopulmonary connection • Computational fluid dynamics • Extracardiac conduit • Stenosis

---

### ABBREVIATIONS

| | |
|---|---|
| 2D | Two-dimensional |
| 3D | Three-dimensional |
| BSA | Body surface area |
| CFD | Computational fluid dynamics |
| CPET | Cardiopulmonary exercise testing |
| CSA | Cross-sectional area |
| CVP | Central venous pressure |
| HV | Hepatic vein |
| IVC | Inferior vena cava |
| LPA | Left pulmonary artery |
| MRI | Magnetic resonance imaging |
| PA | Pulmonary artery |
| PL | Power loss |
| RPA | Right pulmonary artery |
| SVC | Superior vena cava |
| TCPC | Total cavopulmonary connection |

## INTRODUCTION

To complete the Fontan circulation in patients with a univentricular heart defect, most centres nowadays use an extracardiac Goretex conduit of 16–20 mm to connect the inferior vena cava (IVC) with the pulmonary artery (PA) at the age of 2–4 years [1]. However, the synthetic extracardiac conduit lacks growth potential and it is currently unknown if 16-, 18- and 20-mm conduits remain adequately sized for adolescent Fontan patients.

The Fontan circulation is characterized by chronically elevated central venous pressure (CVP) and reduced preload and thereby cardiac output [2]. Efficient blood flow in the total cavopulmonary connection (TCPC) is important to keep the elevation in CVP and reduction in preload to a minimum [3, 4]. Chronic venous hypertension and reduction in preload lead to important morbidity, including liver fibrosis and reduced exercise capacity [1]. Too small conduits are an important factor of increased TCPC resistance and should be avoided [5].

Recently, important blood flow accelerations were observed from the subhepatic IVC towards the conduit 13 years after Fontan completion, indicating that 16–20-mm conduits become relatively undersized for adolescent Fontan patients [6, 16]. However, the haemodynamic consequences of undersized conduits in terms of pressure gradients and TCPC resistance at rest and during simulated exercise were not determined. Therefore, the aim of this study is to determine TCPC haemodynamics using computational fluid dynamics (CFD) in a cohort of teenage and adolescent Fontan patients with 16–20-mm conduits at rest and during simulated exercise and to assess the relationship between conduit size and TCPC haemodynamics.

## METHODS

### Ethical statement

The study was approved by the medical ethical review committee of the hospital (P18.024). Written informed consent was obtained from all patients and/or their parents. Patients and public were not directly involved in the design and conduct of this study.

### Study population

Fontan patients with an extracardiac Goretex conduit prospectively underwent magnetic resonance imaging (MRI) examination between 2018 and 2021 at the Leiden University Medical Center, Leiden, the Netherlands. All patients >8 years old without contraindications for MRI were eligible for inclusion.

### Cardiopulmonary exercise testing

Cardiopulmonary exercise testing (CPET) was performed using a continuous incremental bicycle protocol. Peak $VO_2$ (ml/kg/min) and predicted peak $VO_2$ (%) were determined in all patients with a respiratory exchange ratio >1.0.

## Magnetic resonance imaging

Real-time two-dimensional (2D) flow MRI measurements were obtained at the subhepatic IVC (below entry of the hepatic veins, HVs), at the extracardiac conduit and at the superior vena cava (SVC). HV flow was determined indirectly by subtracting IVC flow from conduit flow. None of the patients had a patent fenestration. Each 2D real-time flow acquisition consisted of 250 (non-electrocardiogram gated) flow measurements with continuously monitoring of the respiratory signal using an air-filled abdominal belt. The respiratory signal was used to divide the flow signal into inspiration and expiration phases as previously described in detail [6].

A three-dimensional (3D) model of the TCPC was created from sagittal and transversal 2D anatomical stacks. Anatomical and 2D real-time flow MRI acquisition details are presented in Supplementary Material, Table S1. The 3D model included the area between the subhepatic IVC, HVs, SVC and right pulmonary artery (RPA) (including the right upper lobe branches) and left pulmonary artery (LPA) up to the level of the segmental branches (ITK-SNAP). The TCPC model was smoothed, centrelines were derived and vessel extensions were added at all inlets and outlets.

## Geometry analysis

The TCPC was automatically divided into standardized segments [conduit, SVC, RPA (distal to right upper lobe branch) and LPA] [7]. The cross-sectional area (CSA) of these segments was determined perpendicular to the centreline at 1-mm intervals from which the mean and minimum CSA was reported. The CSA of the inlet extensions were reported for the subhepatic IVC and HVs. The $CSA_{mean}$ of each vessel was normalized for the respiratory cycle-averaged flow rate ($mm^2$/l/min) in each vessel as a marker of functional vessel CSA.

In addition, the change in measured conduit $CSA_{mean}$ versus theoretical implanted conduit $CSA_{mean}$ was reported (16 mm = 201 $mm^2$, 18 mm = 254 $mm^2$ and 20 mm = 314 $mm^2$).

## Computational fluid dynamics

The 3D TCPC model was meshed with 30 polyhedral elements across the average vessel diameter (0.35–0.45 mm elements) with four prism layers at the wall to achieve mesh-independent results (ANSYS ICEM v17.1, Inc., Canonsburg, PA, USA). All CFD simulations were performed using commercially available Fluent software (v17.1, ANSYS, Inc., Canonsburg, PA, USA). Pulsatile, respiratory cycle-resolved flow rates were prescribed at the inlets using a parabolic velocity profile. Total HV flow was divided over the individual HVs based on the ratio of their respective CSAs. Constant outflow ratios at the PAs were imposed as the outlet boundary condition and subdivided over side branches based on their respective CSAs [8]. The outflow ratio was determined from ECG-gated 2D flow MRI measurements in the PAs since 2D real-time flow measurements in the PAs were not performed. A rigid vessel wall was assumed and a no-slip condition prescribed. Blood flow was assumed to be laminar. A Carreau model was used to account for the non-Newtonian blood properties in the TCPC [9].

## Exercise condition

To simulate the effect of increased flow during exercise on local TCPC haemodynamics, resting flow rates were adapted according to a study by Wei *et al.*, in which 2D real-time flow MRI measurements were obtained during supine lower-leg exercise [10]. The total duration of the respiratory cycle was decreased with a factor of 1.6, the inspiratory fraction (inspiratory time versus total respiration time) was increased with a factor of 1.17 [11] and time-resolved flow rates were increased by a factor of 2.44 (both subhepatic IVC and HVs) and 1.67 (SVC). The resting PA outflow ratios were assumed to remain the same during exercise [12].

## Haemodynamic parameters

***Energetics.*** All parameters were reported during inspiration, expiration and during the entire respiratory cycle. Power loss (PL, in milliwatt) was determined using the viscous dissipation rate method [13]. PL-based pressure gradient (mmHg) from the inlets towards the outlets was determined as follows [8]:

$$\Delta P_{TCPC} = \frac{PL}{Q_s},$$

where PL and $Q_s$ are the total power loss and the total systemic venous return in the corresponding respiratory phase.

The resistance normalized for body surface area (BSA) (in mmHg/l/min/$m^2$) was determined as follows [8]:

$$\text{Normalized resistance} = \frac{\Delta P_{TCPC}}{\frac{Q_s}{BSA}}.$$

***Flow stagnation volume.*** Flow stagnation volume (%) (velocity <0.01 m/s [14]) was determined in a subset of 15 patients as a marker of thrombosis risk; 5 patients per implanted conduit size (16, 18 and 20 mm) matched on average conduit flow rate (range 2.2–4.6 l/min; Supplementary Material, Fig. S1). Minimal (at peak flow during inspiration) and maximal flow stagnation volume (at lowest flow during expiration) were determined in the entire TCPC and in the conduit only. The minimal flow stagnation volume is of particular clinical interest, as this is the volume of blood in the TCPC that remains stagnated during the entire respiratory cycle and theoretically increases the risk of thrombosis.

## Statistical analysis

Data were presented as median (Q1–Q3). Correlation analysis was performed using Pearson (*r*) or Spearman (ρ) correlation (weak 0.3–0.5, moderate 0.5–0.7, strong $\geq$0.7–0.9 and very strong >0.9). Comparison of parameters between respiratory phases and the comparison of $CSA_{mean}$ between TCPC vessels were performed using the Friedman test (adjusted for multiple comparisons using Bonferroni). A comparison of TCPC energetics between gender was made using the Mann–Whitney *U*-test. A comparison of flow stagnation volume between different conduit sizes was determined using the Kruskal–Wallis test. The non-linear relationship between CFD-derived energetics and

normalized conduit CSA was analysed using linear regression after log transformation of both the dependent and independent parameters (power curve). A *P*-value of <0.05 was considered statistically significant. Data were analysed with SPSS 25.0 (IBM Corp., Armonk, NY, USA) and Graphpad Prism 8.0 (GraphPad Software, La Jolla, CA, USA).

## RESULTS

Sixty-five sequential patients underwent MRI examination during the study period. Fourteen/65 patients were excluded because of incomplete 2D real-time MRI flow data ($n = 7$), central device-related artefacts ($n = 3$) or patients with a lateral tunnel Fontan connection ($n = 4$), resulting in 51 patients who were included in this study. Patient characteristics are reported in Table 1. All patients were recruited from the outpatient clinic and were in relatively good clinical condition (NYHA class I–II). CPET was performed in 46/51 patients, with 40 patients reaching maximal effort [median time between CPET and MRI 0 days (Q1–Q3 6–0 days)].

### Geometry and flow

CSA of the different parts of the TCPC is reported in Table 2. Absolute measured conduit $CSA_{mean}$ was 100% (Q1–Q3 94–105), 95% (Q1–Q3 90–106) and 95% (Q1–Q3 72–105) of theoretical implanted conduit size in patients with 16-, 18- and 20-mm conduits, respectively ($P = 0.42$). The conduit $CSA_{mean}$ normalized for conduit flow rate was significantly smaller compared to the normalized $CSA_{mean}$ of all other vessels (all $P < 0.001$); a median 56%, 73% and 64% smaller compared to the subhepatic IVC, HVs and SVC, respectively, and 40% and 35% smaller compared to the LPA and RPA, respectively.

Total systemic venous return during the entire respiratory cycle was 4.5 (Q1–Q3 3.8–5.5) l/min in rest, increasing to 10.8 (Q1–Q3 8.4–12.5) l/min during simulated exercise. Flow rates during inspiration and expiration in the TCPC are reported in Table 2. Flow rates in all vessels were lowest during expiration and highest during inspiration (all $P < 0.001$). Mean conduit flow during the entire respiratory cycle positively correlated with BSA, but considerable variability in flow rates was observed (Fig. 1).

### Energetics

CFD-derived energetics along the respiratory cycle are reported in Table 3, both for resting and simulated exercise conditions. No significant difference in energetics was present between gender.

**Table 1:** Patient characteristics

| | |
|---|---|
| Male/female, *n* | 24/27 |
| Primary diagnosis, *n* (%) | |
|   TA | 12 (24) |
|   HLHS | 9 (17) |
|   DILV + TGA | 10 (20) |
|   DORV | 6 (11) |
|   uAVSD | 3 (6) |
|   ccTGA | 4 (8) |
|   PA + IVS | 2 (4) |
|   Others | 5 (10) |
| Dominant ventricle, *n* (%) | |
|   Left | 30 (59) |
|   Right | 16 (31) |
|   Biventricular/indeterminate | 5 (10) |
| Characteristics at Fontan procedure | |
|   Age at Fontan (years) | 3.3 (2.7–3.9) |
|   Height (cm) | 98 (92–102) |
|   Weight (kg) | 14 (13–16) |
|   BSA (m$^2$) | 0.63 (0.58–0.67) |
|   Implanted conduit size (16/18/20 mm), *n* | 27/18/6 |
|   Fenestration, *n* (%) | 31 (61) |
| Characteristics at time of MRI | |
|   Age at MRI (years) | 16.2 (14.0–18.2) |
|   Height (cm) | 168 (163–175) |
|   Weight (kg) | 59 (50–66) |
|   BSA (m$^2$) | 1.66 (1.52–1.76) |
|   Time between Fontan and MRI (years) | 13.1 (10.4–15.8) |
|   NYHA class I–II, *n* (%) | 51 (100) |
| Cardiopulmonary exercise testing | |
|   RER | 1.11 (1.05–1.17) |
|   Peak Watt | 120 (105–150) |
|   Peak heart rate | 173 (164–184) |
|   Peak predicted heart rate (%) | 94 (86–101) |
|   Peak VO$_2$ (ml/kg/min) | 27.1 (22.4–30.0) |
|   Peak predicted VO$_2$ (%) | 55 (47–65) |

Values are reported as median (Q1–Q3) unless otherwise specified.

BSA: body surface area; ccTGA: congenital corrected transposition of the great arteries; DILV: double inlet left ventricle; DORV: double outlet right ventricle; HLHS: hypoplastic left heart syndrome; IVS: intact ventricular septum; MRI: magnetic resonance imaging; PA: pulmonary artery; RER: respiratory exchange ratio; TA: tricuspid atresia; TGA: transposition of the great arteries; uAVSD: unbalanced atrioventricular septal defect.

**Table 2:** Flow and geometry characteristics

| | Flow (l/min) | | | Geometry | | |
|---|---|---|---|---|---|---|
| | Average respiratory cycle | Inspiration | Expiration | Absolute $CSA_{mean}$ (mm$^2$) | Absolute $CSA_{min}$ (mm$^2$) | Normalized $CSA_{mean}$ (mm$^2$/l/min) |
| Conduit | 3.3 (2.5–4.0) | 4.5 (3.7–5.3) | 2.6 (1.9–3.3) | 217 (199–249) | 196 (182–230) | 65 (54–90) |
| IVC | 1.8 (1.5–2.2) | 2.0 (1.6–2.4) | 1.7 (1.3–2.1) | 263 (222–303) | – | 147 (122–170) |
| HVs | 1.5 (1.0–1.8) | 2.5 (1.8–3.0) | 0.7 (0.5–1.2) | 347 (303–405) | – | 243 (183–352) |
| SVC | 1.3 (1.0–1.6) | 1.5 (1.2–1.8) | 1.2 (1.0–1.5) | 214 (192–262) | 193 (165–224) | 180 (133–216) |
| LPA | 1.9 (1.3–2.3) | 2.5 (1.7–2.9) | 1.5 (1.1–1.9) | 186 (150–236) | 149 (109–192) | 108 (89–153) |
| RPA (distal to RUL branch) | 1.9 (1.5–2.3) | 2.5 (2.0–2.8) | 1.5 (1.1–1.8) | 201 (167–231) | 181 (134–215) | 100 (84–136) |

Data are presented as median (Q1–Q3).

CSA: cross-sectional area; HVs: hepatic veins; IVC: inferior vena cava; LPA: left pulmonary artery; RPA: right pulmonary artery; SVC: superior vena cava; RUL: right upper lobe; NYHA: New York Heart Asssociation; ePTFE: expanded Polytetrafluoroethylene.

## Inspiration versus expiration

During rest, the mean PL was higher during inspiration (median 10.5 mW, Q1–Q3 6.5–14.2) compared to expiration (3.7 mW, Q1–Q3 2.5–6.3, $P < 0.001$). Furthermore, the median pressure gradient was higher during inspiration (0.8 mmHg, Q1–Q3 0.6–1.0) compared to expiration (0.5 mmHg, Q1–Q3 0.4–0.7). No significant difference was present in normalized resistance between inspiration and expiration (Table 3).

## *Rest versus* simulated *exercise*

PL, pressure gradient and normalized resistance all significantly increased from resting to simulated exercise conditions (all $P < 0.001$, Table 3), most pronounced during inspiration for PL and pressure gradient.

A moderate–strong inverse non-linear relationship was present between normalized conduit $CSA_{mean}$ and PL, pressure gradient and normalized resistance, both in rest and simulated exercise conditions (Fig. 2). As derived from the regression curves in Fig. 2B, a normalized conduit $CSA_{mean}$ of $\leq 45$ mm$^2$/l/min corresponded to a median pressure gradient of $\geq 1.0$ at rest and $\geq 3.0$ during simulated exercise. A normalized conduit $CSA_{mean}$ of $\geq 125$ mm$^2$/l/min corresponded to a pressure gradient of $\leq 1.0$ mmHg during both rest and simulated exercise. An example of streamline blood flow visualization and PL heatmaps in 2 Fontan

patients with a small and relatively large normalized conduit $CSA_{mean}$ is illustrated in Fig. 3. Pathline blood flow visualization during 2 respiratory cycles during resting and simulated exercise conditions are shown in Videos 1 and 2.

Furthermore, a negative correlation was present between normalized conduit $CSA_{mean}$ and the relative rest-to-exercise increase in PL ($\rho = -0.63$, $p < 0.001$), pressure gradient ($\rho = -0.59$, $P < 0.001$) and normalized resistance ($\rho = -0.50$, $P < 0.001$), indicating strongest increases in patients with smallest conduits.

Normalized TCPC resistance negatively correlated with peak VO$_2$ (during rest $r = -0.41$, $P = 0.009$ and during simulated exercise $r = -0.37$, $P = 0.020$) and predicted peak VO$_2$ (during rest $r = -0.36$, $P = 0.024$ and during simulated exercise $r = -0.37$, $P = 0.020$, Fig. 4). No correlation was found between PL or pressure gradient and peak VO$_2$ ($r = -0.25$, $P = 0.10$ for both PL and pressure gradient).

## Flow stagnation volume

Minimal (during peak inspiration) and maximal flow stagnation volume (during lowest flow in expiration) in the entire TCPC are reported in Table 3. Minimal flow stagnation volume in the total TCPC was a median of 1.2% (Q1–Q3 0.7–1.8). Increased flow during simulated exercise further reduced minimal flow stagnation volume (median 0.4%, Q1–Q3 0.2–0.7). Minimal flow stagnation volume in the conduit only was absent/negligible (Table 3), with no significant differences between patients with implanted 16-, 18- and 20-mm conduit sizes.

## DISCUSSION

This study shows that extracardiac conduits of 16–20 mm have become undersized in most adolescent Fontan patients on average 13 years after Fontan completion, as evidenced by a significantly smaller normalized conduit $CSA_{mean}$ compared to the other surrounding vessels. Despite this undersizing, pressure gradients in the TCPC were limited (<1 mmHg) during resting conditions in most patients but significantly increased during simulated exercise. Pressure gradients and resistance in the TCPC increased non-linearly with decreasing normalized conduit CSA, and especially patients with a normalized conduit $CSA_{mean} \leq 45$ mm$^2$/l/min showed possibly relevant pressure gradients in the TCPC (>1 mmHg in rest and >3 mmHg during simulated exercise). Finally, a significant correlation was observed between TCPC resistance and (predicted) peak VO$_2$.
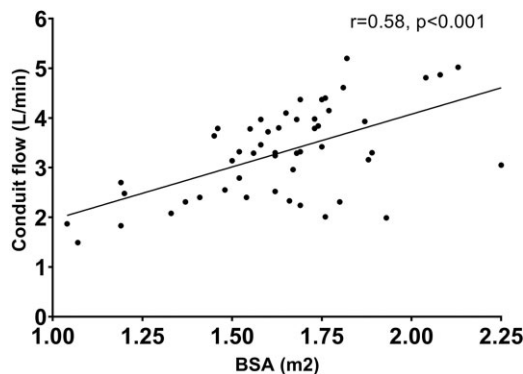


**Figure 1:** A moderate positive correlation is present between BSA and mean conduit flow rate along the entire respiratory cycle. The linear regression line is shown. BSA: body surface area (Haycock).

### Table 3: Computational fluid dynamics results

| Energetics | Resting conditions | | | Exercise conditions | | |
|---|---|---|---|---|---|---|
| | Average | Inspiration | Expiration | Average | Inspiration | Expiration |
| Power loss (mW) | 6.8 (4.1–9.8)[†,‡] | 10.5 (6.5–14.2)[†,§] | 3.7 (2.5–6.3)[†,§] | 48.6 (27.4–70.5)[†,‡] | 61.0 (33.5–86.3)[†,§] | 38.6 (19.0–57.6)[†,§] |
| Pressure gradient (mmHg) | 0.7 (0.5–0.8)[†,‡] | 0.8 (0.6–1.0)[†,§] | 0.5 (0.4–0.7)[†,§] | 2.0 (1.4–2.6)[†,‡] | 2.3 (1.5–2.8)[†,§] | 1.8 (1.2–2.3)[†,§] |
| Normalized resistance (mmHg/l/min/m$^2$) | 0.23 (0.18–0.28)[†,‡] | 0.21 (0.15–0.28)[§] | 0.22 (0.18–0.27)[§] | 0.29 (0.22–0.42)[†] | 0.29 (0.21–0.41)[†] | 0.29 (0.21–0.41)[†,§] |

| Thrombosis marker ($n = 15$) | Minimum (inspiration) | Maximum (expiration) | | Minimum (inspiration) | Maximum (expiration) | |
|---|---|---|---|---|---|---|
| Flow stagnation entire TCPC (%) | 1.2 (0.7–1.8) | 6.2 (4.8–8.0) | | 0.4 (0.2–0.7) | 1.5 (0.8–2.2) | |
| Flow stagnation conduit (%) | 0.0 (0.0–0.0) | 0.5 (0.2–1.2) | | 0.0 (0.0–0.0) | 0.0 (0.0–0.0) | |

Data are presented as median (Q1-Q3). P-value <0.05 compared to inspiration[†], expiration[‡] or the entire respiratory cycle[§].

mW; miliwatt, mmHg; millimeter mercury, L/min; liter/minute. TCPC: total cavopulmonary connection.
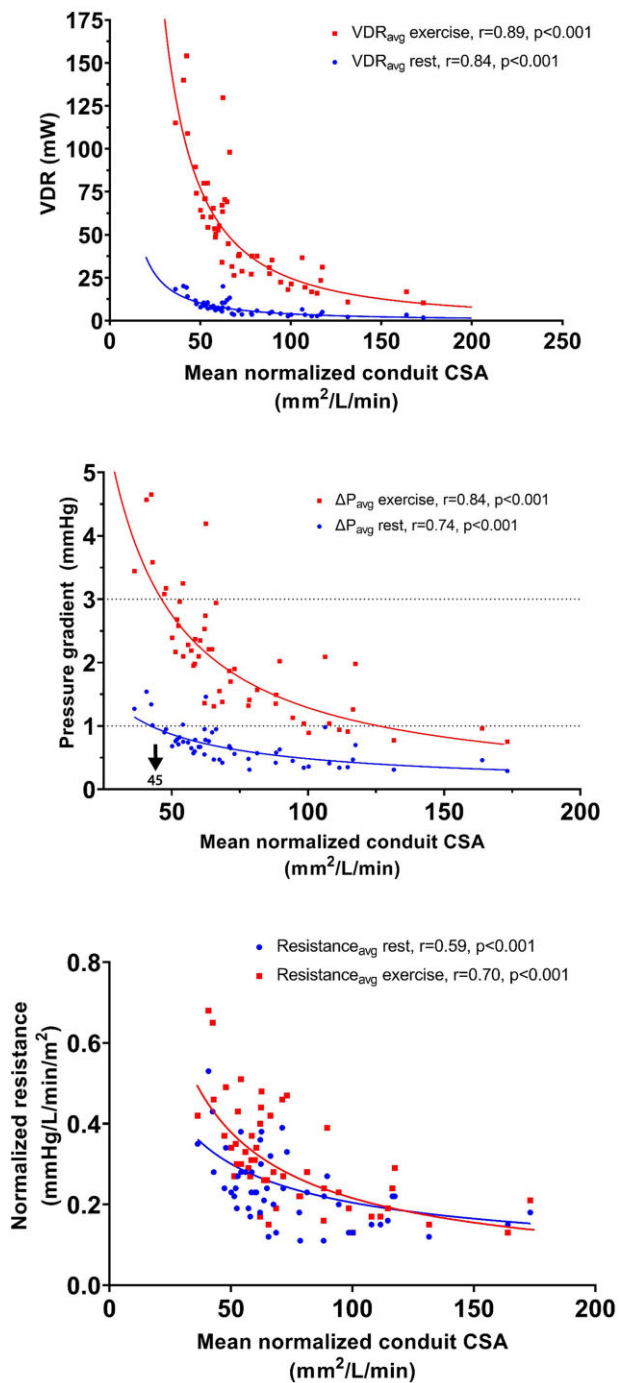
TCPC: total cavopulmonary connection.

**Figure 2:** A moderate-to-strong inverse non-linear relationship is present between power loss (upper panel), pressure gradient (middle panel) and normalized resistance (lower panel) with normalized conduit cross-sectional area, during both rest (blue, lower line) and simulated exercise (red, upper line). One significant outlier of normalized total cavopulmonary connection resistance was excluded from the analysis. CSA: cross-sectional area. (A color version of this figure appears in the online version of this article.)

## Conduit adequacy

The current recommendation is to implant a slightly oversized 16–20-mm extracardiac Goretex conduit in children at the age of 2–4 years, thereby aiming to avoid somatic overgrowth necessitating reintervention [1, 15]. However, optimal conduit size for

adolescent Fontan patients remains elusive mainly because no clear definition is present to describe conduit adequacy. The current study adds important information by assessment of the functional conduit CSA to describe conduit adequacy (conduit $CSA_{mean}$ normalized for conduit flow rate) and by characterizing the associated TCPC haemodynamics.

In our cohort of on average 16-year-old patients with a median conduit flow rate of 3.3 l/min, a median normalized conduit CSA of 65 mm$^2$/l/min was present, significantly smaller compared to the other vessels in the TCPC. For comparison, Itatani *et al.* [14] recommended the use of 16–18-mm conduits for Fontan completion using CFD models based on 36-month-old children with an average conduit flow rate of ∼0.85 l/min in rest. This would correspond to a normalized conduit $CSA_{mean}$ of ∼240–300 mm$^2$/l/min, ∼4–5 times larger to the values reported in our adolescent cohort. Implantation of larger conduits was limited by creating large areas of flow stagnation, potentially increasing the risk of thrombosis. In our study, absent/negligible flow stagnation was present in the conduits, illustrating that there is room for larger conduits in older patients.

## Haemodynamic consequence of conduit undersizing

To assess the haemodynamic consequence of the undersized conduits, we used CFD modelling in rest and during simulated exercise for the quantification of the PL-based pressure gradient and resistance of the TCPC [8]. The ability to simulate blood flow during increased flow conditions (mimicking exercise) is one great advantage of CFD compared to conventional diagnostics such as catheterization, which is usually only limited to resting conditions. This is important, as adverse Fontan haemodynamics may be relatively normal in rest and only become apparent during increased flow conditions [17, 18]. The use of CFD-simulated exercise showed that pressure gradients were relatively low (<1 mmHg) in rest but significantly increased during simulated exercise to values of >1–5 mmHg. These data therefore emphasize the current drawbacks of evaluating TCPC haemodynamics using catheterization in rest, as small pressure gradients in rest may mask potential relevant pressure gradients during exercise.

## Clinical relevance of total cavopulmonary connection pressure gradients

Any raise in TCPC pressure gradient during resting conditions will chronically elevate CVP, and recently an elevated TCPC resistance has been associated with increased levels of liver fibrosis [19]. Therefore, TCPC pressure gradients of 1–1.5 mmHg in rest in patients with the smallest conduits may lead to increased progression of liver fibrosis, as is observed in extracardiac conduit compared to lateral tunnel Fontan patients [20].

During exercise, an increase in CVP is limited to values of on average 20–23 mmHg to augment blood flow towards the single ventricle [18, 21, 22]. Therefore, increased resistance and pressure gradients in the TCPC will come at the expense of reduced preload towards the single ventricle when the upper limit of the CVP is reached. Systemic venous hypertension during exercise in Fontan patients has been linked to adverse clinical outcome and exercise capacity [21, 22]. In this light, TCPC pressure gradients of
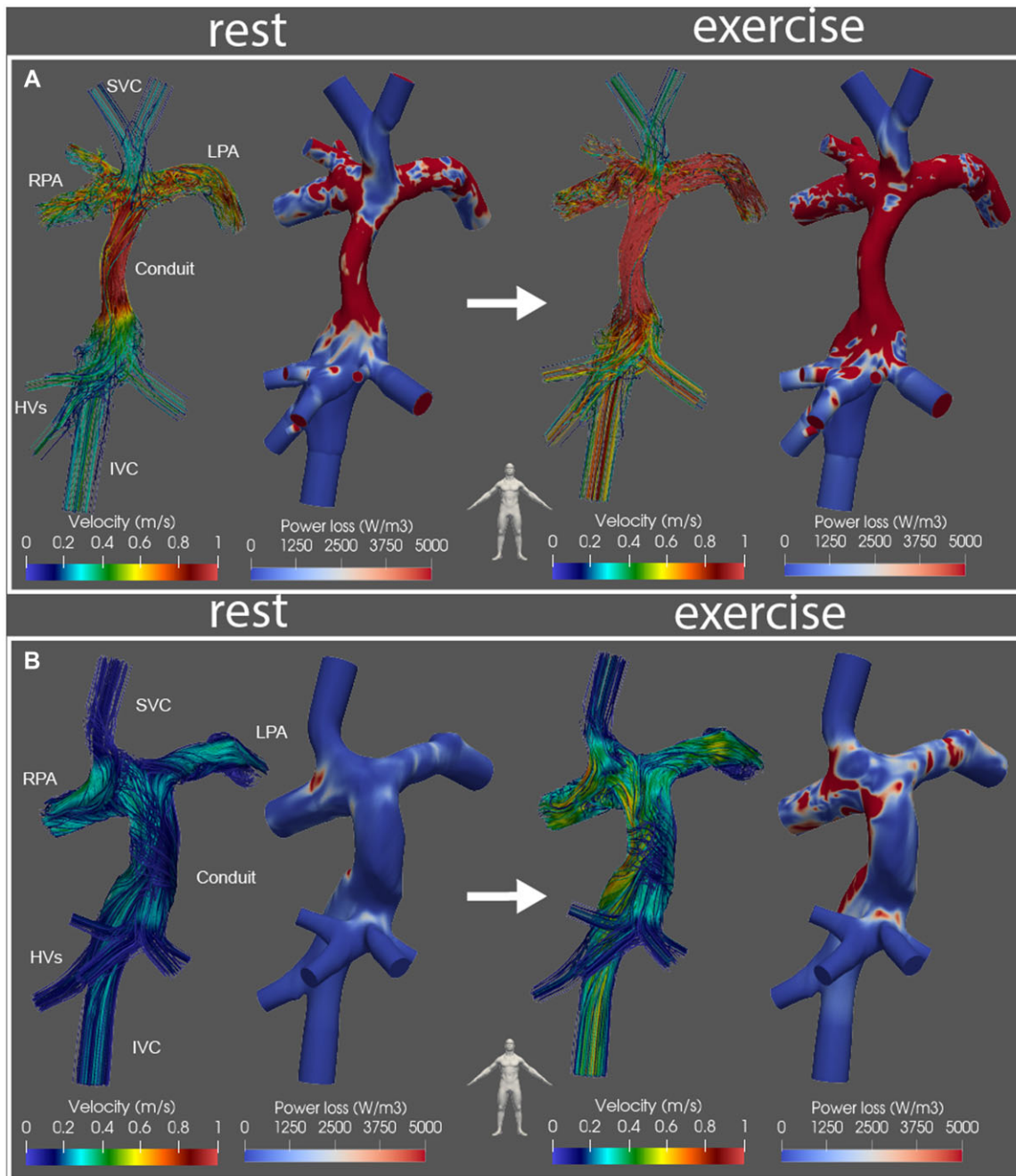
**Figure 3:** Velocity-coloured streamline representation and power loss heatmaps of blood flow in the total cavopulmonary connection during peak inspiration is shown for 2 Fontan patients with a relatively small (**A**) and large (**B**) normalized conduit $CSA_{mean}$. Note the strong increase in blood flow velocity and power loss at the junction between the IVC/HVs and the extracardiac conduit extending into the pulmonary arteries in patient A, indicating the presence of an functionally undersized conduit. Patient A: 16 years, body surface area 1.82 m$^2$, 16-mm conduit, mean conduit flow respiratory cycle 5.2 l/min, normalized conduit $CSA_{mean}$ 36 mm$^2$/l/min. Computational fluid dynamic energetics (rest/exercise): power loss 18.3/115.1 mW, pressure drop 1.3/3.4 mmHg, normalized resistance 0.35/0.41 mmHg/l/min/m$^2$. Patient B: 16 years, body surface area 1.76 m$^2$, 20-mm conduit, mean conduit flow respiratory cycle 2.0 l/min, normalized conduit $CSA_{mean}$ 173 mm$^2$/l/min. Computational fluid dynamic energetics (rest/exercise): power loss 1.7/10.3 mW, pressure drop 0.3/0.8 mmHg, normalized resistance 0.18/0.21 mmHg/l/min/m$^2$. CSA: cross-sectional area; HVs: hepatic veins; IVC; inferior vena cava; SVC; superior vena cava.

2–5 mmHg during simulated exercise may be of significant magnitude leading to suboptimal exercise haemodynamics.

Currently, no cut-off values for clinically relevant pressure gradients in the TCPC are defined that may indicate the need for intervention, but catheterization-derived pressure gradients as low as 1 mmHg are already considered as a clinically relevant Fontan pathway obstruction [23]. Our data indicate that patients with a conduit of ≤45 mm$^2$/l/min may require close monitoring,

as further decline in functional conduit size is expected to lead to a non-linear increase in pressure gradient and resistance. A recent study showed that dilatation and stenting of the conduit improved haemodynamics and functional status, exclusively in patients with low ventricular end-diastolic pressure <10 mmHg [24]. Of note, our study analysed the performance of extracardiac conduits in adolescents that become undersized due to somatic growth and did not include patients with an important localized
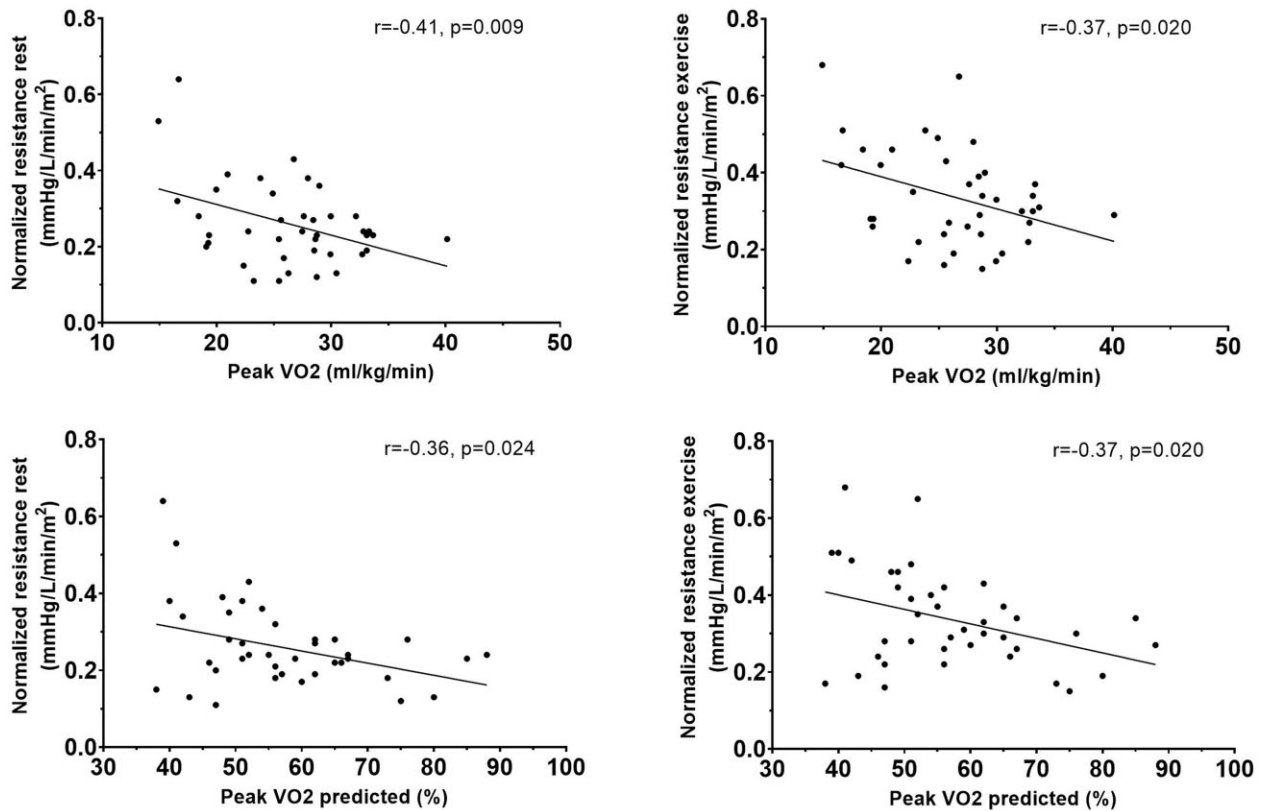
**Figure 4:** A weak inverse linear correlation is observed between normalized resistance of the total cavopulmonary connection and peak $VO_2$ (upper panels) and predicted peak $VO_2$ (lower panels) in rest (left panels) and during simulated exercise (right panels).

stenosis. Energy losses and pressure gradients will be further elevated when a significant localized narrowing is present.

## Relevance for future surgical strategy

Favourable haemodynamics (pressure gradient <1 mmHg during both rest and exercise) were observed in patients with a conduit CSA of $\geq$125 mm$^2$/l/min, which could be the 'ideal' conduit size to aim for an adult age and is approximately in line with values observed in the other TCPC vessels. This corresponds to conduit sizes of between 375 mm$^2$ (i.e. ±22 mm) and 625 mm$^2$ (±28 mm) for patients with 3–5 l/min conduit flow during rest, in line with suprahepatic IVC diameters observed in healthy persons [25] and with lateral tunnel CSA (420–580 mm$^2$, i.e. 23–27 mm) observed in 10- to 15-year-old Fontan patients [6, 26, 27]. However, implanting larger conduit sizes at the initial Fontan operation is not feasible due to anatomical constraints, including potential pulmonary vein obstruction, risk of subsequent PA distortion and the increased risk of conduit thrombosis [14, 28]. Based on our observations, in our opinion, alternative surgical strategies should be explored such as implanting other, non-rigid materials including dilatable ePTFE grafts (e.g. PECA labs) or the use of tissue-engineered grafts with growth potential [29].

## Limitations

Flow rates were modelled with respect to the respiratory cycle, ignoring the effect of the cardiac cycle on flow rates. However, since flow pulsatility is almost entirely related to the respiratory

cycle [30, 31], inaccuracies are likely small. Regarding the exercise modelling, no patient-specific exercise flow data were available necessitating the use of cohort-averaged increases in flow from rest to exercise. Furthermore, the effects of exercise on other components of the cardiovascular system were not taken into account, which would require more complex, multiscale models [32], limiting our analysis to the analysis of local TCPC haemodynamics only.

The measured conduit CSA$_{mean}$ exceeded the theoretical conduit CSA in some patients and this overestimation might be related to limited resolution of the MRI acquisition. Lastly, the potential improvement in TCPC haemodynamics with larger conduits was not studied. CFD models using virtual surgery could be useful to determine the potential improvement in TCPC haemodynamics with the implantation of larger conduit sizes.

## CONCLUSIONS

Extracardiac conduits of 16–20 mm have become relatively undersized in most adolescent Fontan patients. Pressure gradients and resistance in the TCPC increased non-linearly with decreasing normalized conduit CSA and a significant correlation was observed between normalized TCPC resistance and peak $VO_2$. Fontan completion using alternative conduit materials should be explored to further optimize haemodynamics in adolescent Fontan patients.

## SUPPLEMENTARY MATERIAL

Supplementary material is available at *EJCTS* online.
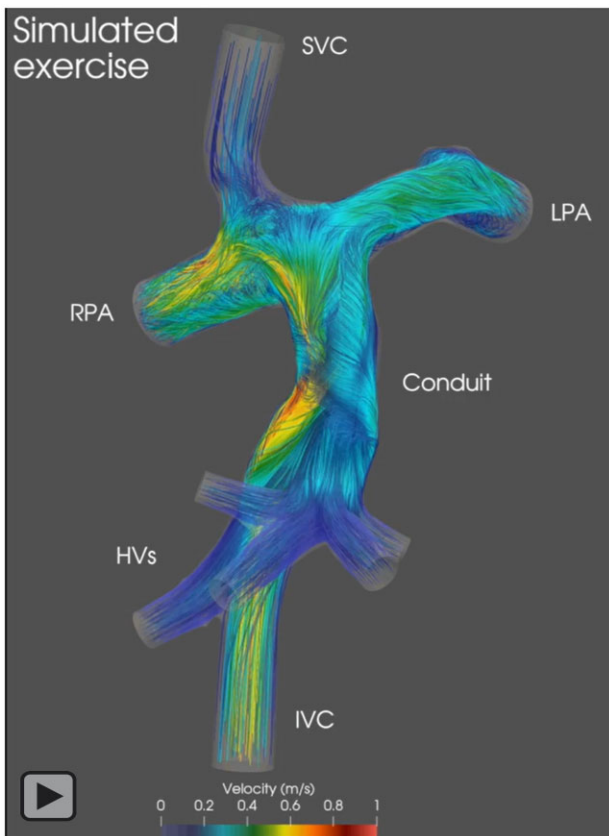
**Video 1:** Velocity-coloured pathline representation of blood flow in the total cavopulmonary connection during 2 respiratory cycles in rest and simulated exercise is shown for a Fontan patient with a large functional conduit size (normalized conduit $CSA_{mean}$ 173 mm$^2$/l/min). Note how during early expiration backflow/flow stagnation is present during rest, disappearing during inspiration. No significant acceleration in blood flow from the IVC towards the conduit is present in rest and during exercise. CSA: cross-sectional area; IVC; inferior vena cava.

## Funding

**Conflict of interest:** none declared.

## Data availability statement

Data are available on reasonable request.

## Author contributions

**Friso M. Rijnberg:** Conceptualization; Data curation; Formal analysis; Funding acquisition; Investigation; Methodology; Project administration; Resources; Visualization; Writing—original draft. **Luca C. van 't Hul:** Formal analysis; Methodology; Writing—review & editing. **Mark G. Hazekamp:** Supervision; Writing—review & editing. **Pieter J. van den Boogaard:** Data curation; Writing—review & editing. **Joe F. Juffermans:** Investigation; Software; Writing—review & editing. **Hildo J. Lamb:** Resources; Writing—review & editing. **Covadonga Terol Espinosa de Los Monteros:** Formal analysis; Writing—review & editing. **Lucia J.M. Kroft:** Resources; Writing—review & editing. **Sasa Kenjeres:** Investigation; Methodology; Writing—review & editing. **Saskia le Cessie:** Formal analysis; Methodology; Writing—review & editing. **Monique R.M. Jongbloed:** Writing—review & editing. **Jos J.M. Westenberg:** Conceptualization; Resources; Supervision; Writing—review & editing. **Arno
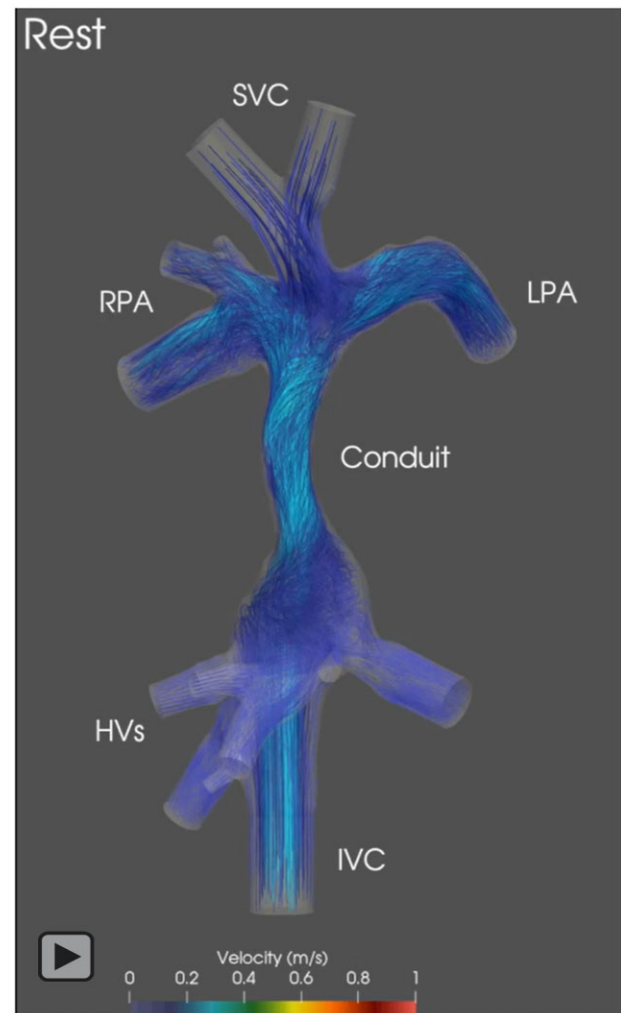


**Video 2:** Velocity-coloured pathline representation of blood flow in the total cavopulmonary connection during 2 respiratory cycles in rest and simulated exercise is shown for a Fontan patient with a small functional conduit size (normalized conduit $CSA_{mean}$ 36 mm$^2$/l/min). Note the strong increase in blood flow velocity at the junction between the IVC/HVs and the extracardiac conduit extending into the PAs in rest, indicating the presence of a functionally undersized conduit. During early expiration, IVC-to-conduit flow acceleration is modest but significantly increases during inspiration reaching up into the superior vena cava, further augmented during simulated exercise. CSA: cross-sectional area; HVs: hepatic veins; IVC; inferior vena cava; PAs: pulmonary arteries.

**A.W. Roest:** Conceptualization; Investigation; Methodology; Supervision; Writing—review & editing. **Jolanda J. Wentzel:** Conceptualization; Investigation; Methodology; Resources; Software; Supervision; Writing—review & editing.

## Reviewer information

## REFERENCES

[1] Rychik J, Atz AM, Celermajer DS, Deal BJ, Gatzoulis MA, Gewillig MH et al; On behalf of the American Heart Association Council on Cardiovascular Disease in the Young and Council on Cardiovascular and

Stroke Nursing. Evaluation and management of the child and adult with Fontan circulation: a scientific statement from the American Heart Association. Circulation 2019;140:CIR0000000000000696.

[2] Gewillig M, Brown SC. The Fontan circulation after 45 years: update in physiology. Heart 2016;102:1081–6.

[3] Rijnberg FM, Hazekamp MG, Wentzel JJ, de Koning PJH, Westenberg JJM, Jongbloed MRM et al Energetics of blood flow in cardiovascular disease: concept and clinical implications of adverse energetics in patients with a Fontan circulation. Circulation 2018;137:2393–407.

[4] Sundareswaran KS, Pekkan K, Dasi LP, Whitehead K, Sharma S, Kanter KR et al The total cavopulmonary connection resistance: a significant impact on single ventricle hemodynamics at rest and exercise. Am J Physiol Heart Circ Physiol 2008;295:H2427–35.

[5] Tang E, Restrepo M, Haggerty CM, Mirabella L, Bethel J, Whitehead KK et al Geometric characterization of patient-specific total cavopulmonary connections and its relationship to hemodynamics. JACC Cardiovasc Imaging 2014;7:215–24.

[6] Rijnberg FM, van der Woude SFS, Hazekamp MG, van den Boogaard PJ, Lamb HJ, Terol Espinosa de Los Monteros C et al Extracardiac conduit adequacy along the respiratory cycle in adolescent Fontan patients. Eur J Cardiothorac Surg 2022;62.

[7] Rijnberg FM, Juffermans JF, Hazekamp MG, Helbing WA, Lamb HJ, Roest AAW et al Segmental assessment of blood flow efficiency in the total cavopulmonary connection using 4D flow MRI: vortical flow is associated with increased viscous energy loss. Eur Heart J Open 2021;1: oeab018.

[8] Haggerty CM, Restrepo M, Tang E, de Zelicourt DA, Sundareswaran KS, Mirabella L et al Fontan hemodynamics from 100 patient-specific cardiac magnetic resonance studies: a computational fluid dynamics analysis. J Thorac Cardiovasc Surg 2014;148:1481–9.

[9] Wei Z, Singh-Gryzbon S, Trusty PM, Huddleston C, Zhang Y, Fogel MA et al Non-Newtonian effects on patient-specific modeling of Fontan hemodynamics. Ann Biomed Eng 2020;48:2204–17.

[10] Wei Z, Whitehead KK, Khiabani RH, Tree M, Tang E, Paridon SM et al Respiratory effects on Fontan circulation during rest and exercise using real-time cardiac magnetic resonance imaging. Ann Thorac Surg 2016; 101:1818–25.

[11] Hjortdal VE, Emmertsen K, Stenbog E, Frund T, Schmidt MR, Kromann O et al Effects of exercise and respiration on blood flow in total cavopulmonary connection: a real-time magnetic resonance flow study. Circulation 2003;108:1227–31.

[12] Khiabani RH, Whitehead KK, Han D, Restrepo M, Tang E, Bethel J et al Exercise capacity in single-ventricle patients after Fontan correlates with haemodynamic energy loss in TCPC. Heart 2015;101:139–43.

[13] Wei ZA, Tree M, Trusty PM, Wu W, Singh-Gryzbon S, Yoganathan A. The advantages of viscous dissipation rate over simplified power loss as a Fontan hemodynamic metric. Ann Biomed Eng 2018;46:404–16.

[14] Itatani K, Miyaji K, Tomoyasu T, Nakahata Y, Ohara K, Takamoto S et al Optimal conduit size of the extracardiac Fontan operation based on energy loss and flow stagnation. Ann Thorac Surg 2009;88:565–72; discussion 72–3.

[15] Daley M, d'Udekem Y. The optimal Fontan operation: lateral tunnel or extracardiac conduit? J Thorac Cardiovasc Surg 2020;162(6):1825–1834.

[16] Rijnberg FM, van Assen HC, Hazekamp MG, Roest AAW, Westenberg JJM. Hemodynamic consequences of an undersized extracardiac conduit in an adult Fontan patient revealed by 4-dimensional flow magnetic resonance imaging. Circ Cardiovasc Imaging 2021;14:e012612.

[17] Egbe AC, Miranda WR, Anderson JH, Borlaug BA. Hemodynamic and clinical implications of impaired pulmonary vascular reserve in the Fontan circulation. J Am Coll Cardiol 2020;76:2755–63.

[18] Van De Bruaene A, La Gerche A, Claessen G, De Meester P, Devroe S, Gillijns H et al Sildenafil improves exercise hemodynamics in Fontan patients. Circ Cardiovasc Imaging 2014;7:265–73.

[19] Trusty PM, Wei ZA, Rychik J, Graham A, Russo PA, Surrey LF et al Cardiac magnetic resonance-derived metrics are predictive of liver fibrosis in Fontan patients. Ann Thorac Surg 2020;109:1904–11.

[20] Evans WN, Acherman RJ, Mayman GA, Galindo A, Rothman A, Winn BJ et al The rate of hepatic fibrosis progression in patients post-Fontan. Pediatr Cardiol 2020;41:905–9.

[21] Colman K, Alsaied T, Lubert A, Rossiter HB, Mays WA, Powell AW et al Peripheral venous pressure changes during exercise are associated with adverse Fontan outcomes. Heart 2021;107:983–8.

[22] Ono S, Yanagi S, Wakamiya T, Ichikawa Y, Kawai S, Kim KS et al Correlation of exercise-induced peripheral venous hypertension with exercise intolerance in patients with Fontan circulation. Cardiol Young 2022;32:1427–31.

[23] Alsaied T, Rathod RH, Aboulhosn JA, Budts W, Anderson JB, Baumgartner H et al Reaching consensus for unified medical language in Fontan care. ESC Heart Fail 2021;8(5):3894–3905.

[24] Hagler DJ, Miranda WR, Haggerty BJ, Anderson JH, Johnson JN, Cetta F et al Fate of the Fontan connection: mechanisms of stenosis and management. Congenit Heart Dis 2019;14:571–81.

[25] Ettinger E, Steinberg I. Angiocardiographic measurement of the cardiac segment of the inferior vena cava in health and in cardiovascular disease. Circulation 1962;26:508–15.

[26] Bossers SSM, Cibis M, Gijsen FJ, Schokking M, Strengers JLM, Verhaart RF et al Computational fluid dynamics in Fontan patients to evaluate power loss during simulated exercise. Heart 2014;100:696–701.

[27] Restrepo M, Mirabella L, Tang E, Haggerty CM, Khiabani RH, Fynn-Thompson F et al Fontan pathway growth: a quantitative evaluation of lateral tunnel and extracardiac cavopulmonary connections using serial cardiac magnetic resonance. Ann Thorac Surg 2014;97:916–22.

[28] Alexi-Meskishvili V, Ovroutski S, Ewert P, Dahnert I, Berger F, Lange PE et al Optimal conduit size for extracardiac Fontan operation. Eur J Cardiothorac Surg 2000;18:690–5.

[29] Szafron JM, Ramachandra AB, Breuer CK, Marsden AL, Humphrey JD. Optimization of tissue-engineered vascular graft design using computational modeling. Tissue Eng Part C: Methods 2019;25:561–70.

[30] Gabbert DD, Hart C, Jerosch-Herold M, Wegner P, Salehi Ravesh M, Voges I et al Heart beat but not respiration is the main driving force of the systemic venous return in the Fontan circulation. Sci Rep 2019;9: 2034.

[31] van der Woude SFS, Rijnberg FM, Hazekamp MG, Jongbloed MRM, Kenjeres S, Lamb HJ et al The influence of respiration on blood flow in the fontan circulation: insights for imaging-based clinical evaluation of the total cavopulmonary connection. Front Cardiovasc Med 2021;8: 683849.

[32] Hsia T-Y, Figliola R, Bove E, Dorfman A, Taylor A et al; Investigators obotMoCHA. Multiscale modelling of single-ventricle hearts for clinical decision support: a Leducq Transatlantic Network of Excellence. Eur J Cardiothorac Surg 2016;49:365–8.